Biointerface Research in Applied Chemistry
Open-Access Journal (ISSN: 2069-5837)

Article
Volume 13, Issue 4, 2023, 346
https://doi.org/10.33263/BRIAC134.346

Investigating a Boron Nitride Plate for the Formaldehyde Adsorption: Density Functional Theory Calculations

Kun Harismah [1,*], Maadh Fawzi Nassar [2,3], Omar Talal Hamid [4], Mohsin O. AL-Khafaji [5], Hasan Zandi [6,*]

1 Department of Chemical Engineering, Faculty of Engineering, Universitas Muhammadiyah Surakarta, Surakarta, Indonesia; kun.harismah@ums.ac.id (K.H.);
2 Integrated Chemical BioPhysics Research, Faculty of Science, Universiti Putra Malaysia, 43400 UPM Serdang, Selangor, Malaysia; nassarmaadh@gmail.com (M.F.N.);
3 Department of Chemistry, Faculty of Science, Universiti Putra Malaysia, 43400 UPM Serdang, Selangor, Malaysia; nassarmaadh@gmail.com (M.F.N.);
4 Department of Oil and Gas Refining Engineering, Al-Turath University College, Baghdad, Iraq; omar.talal@turath.edu.iq (O.T.H.);
5 Air Conditioning and Refrigeration Techniques Engineering Department, Al-Mustaqbal University College, Babylon 51001, Iraq; mohsen-aleiwi@mustaqbal-college.edu.iq (M.O.A.);
6 Department of Chemistry, Faculty of Science, University of Qom, Qom, Iran; h.zandi.dr@gmail.com (H.Z.);
* Correspondence: kun.harismah@ums.ac.id (K.H.); h.zandi.dr@gmail.com; (H.Z.);
Scopus Author ID 56982926300 (K.H.); 14122606900 (H.Z.);
Received: 24.06.2022; Accepted: 17.07.2022; Published: 17.09.2022

Abstract: A boron nitride (BN) plate was investigated in this work for adsorbing the formaldehyde (Frm) substance by performing the density functional theory (DFT) calculations. The singular models of BN and Frm were optimized first, and their combinations were re-optimized next to obtain Frm@BN complexes; F1 and F2 were found. To manage the interaction processes, an iron (Fe) atom was inserted in the center of a small plate. The results showed the benefits of such atomic insertion for approaching the goal of this work. Details of interactions were analyzed, and the results show the existence of two interactions for each of obtained Frm@BN bimolecular models. The model with O…Fe, and H…N interactions (F1) was placed at a higher level of strength than the model with the existence of H…Fe and H…N interactions (F2). Accordingly, energy levels of characteristic frontier molecular orbitals and their related features affirmed the impacts of complex formations leading to the possibility of running diagnostic processes. Additionally, the role of the Fe-doped region was dominant in conducting the adsorption processes, and the results of both F1 and F2 complexes revealed such importance. Consequently, the stabilized models regarding the energies and interactions details affirmed this achievement for proposing the formations of Frm@BN complexes for environmental applications.

Keywords: boron nitride; nanostructure; formaldehyde; adsorption; computational study.

1. Introduction

Soon after the nanostructures innovation, assessments of their features showed the benefits of employing novel structures for conducting adsorption [1-5]. Accordingly, various functions and applications have been expected for the nanostructures from biological systems up to industrial fields [6-10]. Besides the pioneering carbon nanotubes (CNTs), several other nanostructures have been innovated with characteristic features of wide surface area for adsorbing other substances [11-15]. Moreover, non-carbon-based nanostructures are even better than pure carbon nanostructures for participating in efficient adsorption processes [16-

20]. Combinations of boron and nitrogen atoms led to the innovation of boron nitride (BN) nanostructures with heteroatomic surfaces compared with the homoatomic composition of carbon nanostructures [21]. Additionally, different values of electronegativity of boron and nitrogen atoms provided almost an ionic surface for the BN nanostructures [22]. Several shapes of these BN-related nanostructures have been known this time, including planar, tubular, conical, spherical, linear, and other geometrical shapes [23-25]. Interestingly, the BN nanostructures are always supposed to be semiconductors in contrast with carbon nanostructures' metallic and semiconductor features [26-28]. Accordingly, investigating sensor features of BN nanostructures has been found important for specifying their applications in diagnostic situations [29]. Considerable efforts have been dedicated to recognizing nanostructures' benefits for diagnosing pollutants, conducting drug delivery platforms, and other related adsorption processes [30-35].In this regard, the BN nanostructures have been seen as useful for adsorbing other substances, such as gaseous molecules or pharmaceutical substances [36-38]. Within the current computational work, a representative BN plate was investigated for formaldehyde (Frm) adsorption (Figure 1) to learn about details of the adsorption process besides learning the benefits of this application for environmental issues. It is worth mentioning that investigating health-related topics are always at the highest levels of importance because of the need to marinate the living systems' stability and safety [39-43].

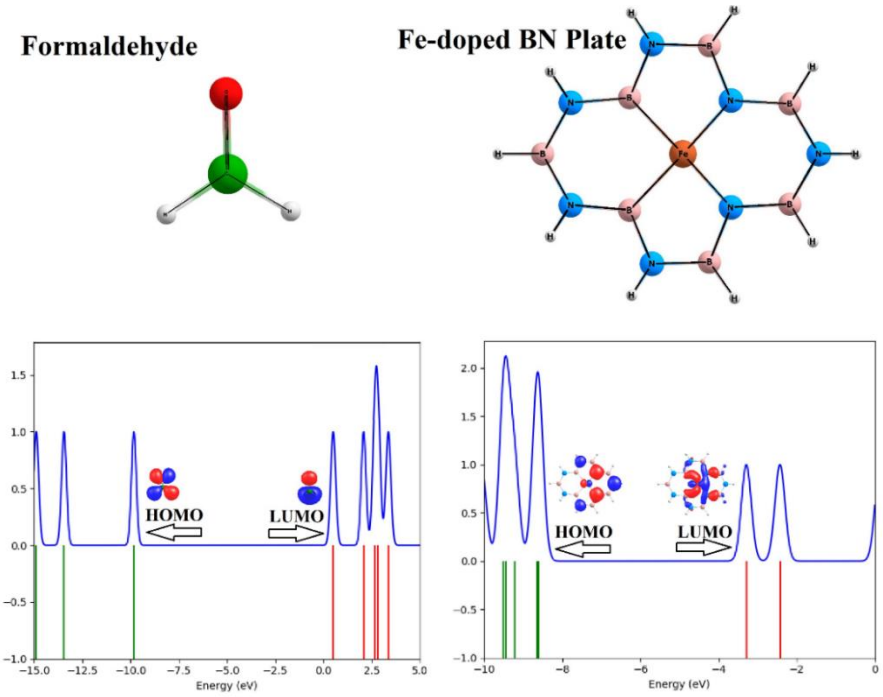

Figure 1. Optimized Frm and BN models and their HOMO-LUMO patterns and DOS diagrams.

Formaldehyde (CH_2O) is one of the essential chemical compounds of several industries; in which it can be stored in liquid form, but it is naturally a low-boiling-point gas [44]. Although it should be equipped for industrial processes, its exhaustion to the environment could cause dangers to the health of living systems [45-47]. In this case, formaldehyde has also been known as a pollutant with recognition and elimination importance for saving the living systems [48]. Accordingly, considerable attempts have been dedicated to innovative adsorbents for such small gaseous molecules regarding environmental issues [49-51]. Indeed, exploring determination tools is very important in various fields especially for health issues [52-54]. Earlier works reported the benefits of employing nanostructures for conducting the adsorption

of formaldehyde in different conditions [55]. To approach the goal of innovation of new adsorption system, computational tools have been very useful to generate the required information at the smallest scale of interacting substances [56-60]. Based on such achievements, this work was performed by employing computational tools for investigating a BN plate for the adsorption of formaldehyde [61]. To provide an active site of interactions, an iron (Fe) was instated in the central position of the plate to make a Fe-doped region for targeted interaction with the formaldehyde substance. Indeed, the atomic dopants could manage targeted interactions for the surfaces towards other substances [62-66]. The investigating molecular models of this work were optimized, and their characterizing features were evaluated to assess the formaldehyde adsorption by the BN plate (Tables 1 and 2 and Figures 1 and 2).

2. Materials and Methods

As shown in Figure 1, the original models of this work were molecules of formaldehyde (Frm) (CH_2O) and Fe-doped BN plate ($B_7N_7H_{10}Fe$), in which their combinations were investigated to obtain the interacting bimolecular models of Frm@BN complexes (Figure 2). Indeed, the Fe-doped region was an active site of interactions for the BN plate to participate in interactions with the Frm substance. All possibilities of bimolecular model formations were examined by initiating interactions with various configurational positions of Frm and BN towards each other, resulting in two Frm@BN complexes; F1 and F2. The optimization calculations of bimolecular models were performed without any restriction to obtain the geometrically minimized models. Additionally, the analyses of the quantum theory of atoms in molecules (QTAIM) were performed to recognize details of interactions and strengths for forming Frm@BN complexes. Besides interaction details of bimolecular models (Table 1), other details, including various types of energies, were listed in Table 2. Moreover, graphical representations of optimized models, frontier molecular orbitals distribution patterns, and diagrams of the density of states (DOS) were exhibited in Figures 1 and 2. All calculations of this work were done by the wB97XD/6-31+G* level of density functional theory (DFT) as implemented in the Gaussian program [67].

3. Results and Discussion

This computational work was done to investigate a BN plate for the Frm adsorption regarding environmental issues. To this aim, a representative model of Fe-doped BN plate was used to adsorb the Frm molecule through optimization processes of DFT calculations. Optimized forms of the singular Frm and BN models and the bimolecular Frm@BN models are shown in Figures 1 and 2. As could be seen by the models, stabilized structures were found, and their features were evaluated (Tables 1 and 2). Examining the results of singular models could show that the models were in the good mode of electron transferring contributions because of their different energy values of characteristic frontier molecular orbitals; HOMO and LUMO levels. It should be noted that the highest occupied molecular orbital (HOMO) and the lowest unoccupied molecular orbital (LUMO) stand for the most achievable levels of electron transferring in the molecular models. Accordingly, the idea of formations of such Frm@BN bimolecular complexes could be supported by such different levels of HOMO and LUMO and their possibility of participating in electron transfer processes. To this aim, the already optimized singular models of Frm and BN were combined with each other through performing re-optimization calculations to yield the stabilized Frm@BN bimolecular models.

As the Fe-doped region of the BN plate was indeed an active site of interactions, the Frm substance was relaxed mainly towards this atomic site in both obtained F1 and F2 complexes (Figure 2). Next, details of interactions and strengths were examined by performing the QTAIM analyses of bimolecular models. The results were summarized in Table 1 to show the types and distances of interactions, total electron density (Rho), Laplacian of electron density (Del^2-Rho), and energy of electron density (H) for describing the interacting bimolecular complexes [68-70].

Table 1. QTAIM features of Frm@BN models.[1]

Frm@BN Model	Interaction	Distance (Å)	Rho (au)	Del^2-Rho (au)	H (au)
F1	O…Fe	1.97	0.0678	0.5069	-0.0658
	H…N	2.83	0.0061	0.0221	-0.0011
F2	H…Fe	1.83	0.0443	0.1154	-0.0137
	H…N	2.82	0.0067	0.0224	-0.0098

[1]The models are shown in Figures 1 and 2.

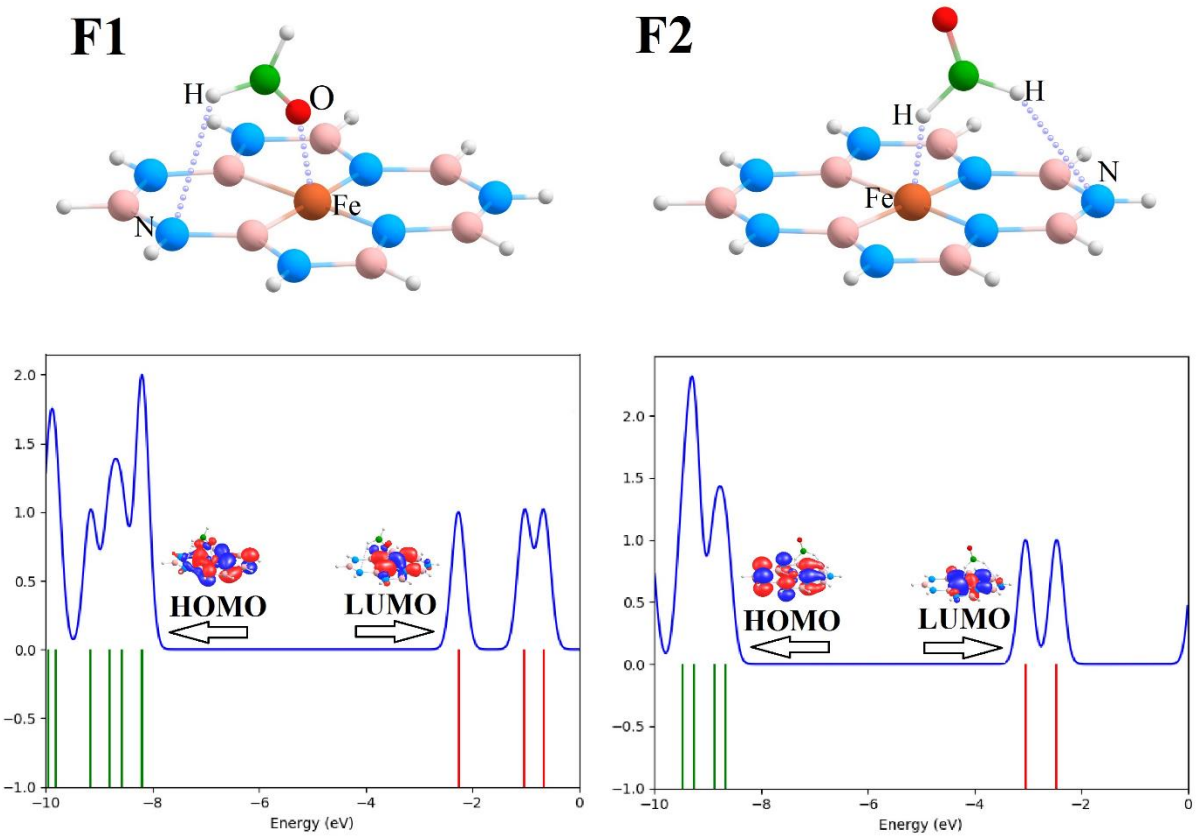

Figure 2. Optimized Frm@BN models and their HOMO-LUMO patterns and DOS diagrams.

For each of the two configurations of Frm@BN bimolecular models, two interactions were found; O…Fe and H…N for F1 and H…Fe and H…N for F2. It was found that the Fe-doped region managed the two-leg interactions of Frm with involvement in interactions in both of F1 and F2 models. The obtained QTAIM features indicated reasonable electronic conditions for the occurrence of interactions between two molecule models. The O…Fe type of interaction was found to be at the highest strength compared to other interactions; the H…Fe and H…N types were placed at the next orders. All the obtained values of Rho, Del^2-Rho, and H of Table 1 affirmed occurrences of two meaningful interactions for both of F1 and F2 models. In this regard, the idea of the formation of Frm@BN complexes was confirmed.

Further analyses of the models were done with the assistance of the evaluated energy features of the models, as summarized in Table 2. First, the value of E_{Ads}; representing the

adsorption energy, showed meaningful strengths for formations of both F1 and F2 complexes. Additionally, the strength of F1 was found higher than F2, remembering the role of O…Fe interaction in forming this complex model. The exact values of obtained E_{Ads} were -30.66 kcal/mol and -10.12 kcal/mol for F1 and F2, respectively.

Table 2. Energy features of Frm, BN, and Frm@BN models.[1]

Model	E_{Ads} (kcal/mol)	HOMO (eV)	LUMO (eV)	E_{Gap} (eV)	E_{Fermi} (eV)	CH (eV)	CS (eV^{-1})
Frm	n/a	-9.82	0.50	10.33	-4.66	5.16	0.19
BN	n/a	-8.60	-3.29	5.31	-5.95	2.66	0.38
F1	-30.66	-8.18	-2.26	5.92	-5.22	2.96	0.34
F2	-10.12	-8.67	-3.04	5.62	-5.85	2.81	0.36

[1]The models are shown in Figures 1 and 2.

Other obtained energy features were for HOMO and LUMO levels standing for the levels of electron transferring in forming bimolecular models. As shown by the evaluated HOMO-LUMO distribution patterns and DOS diagrams (Figures 1 and 2), the energy values of HOMO-LUMO levels of singular models were different. The observation helped to approach the idea of the occurrence of interactions in two singular models. Moreover, the LUMO level of the singular BN plate was mainly localized at the Fe-doped region to show the role of such modification for better adsorbing other substances. Accordingly, formations of bimolecular models led to the relaxation of two configurations of Frm and BN towards each other, in which the O-leg of Frm was placed towards the Fe-doped region in F1 (O…Fe), and the H-leg of Frm was placed towards the Fe-doped region in F2 (H…Fe). In both F1 and F2 models, one additional H…N interaction was also observed. In such cases, the obtained results of HOMO-LUMO showed impacts on complex formations, showing different results between singular and biomolecular forms and even between two bimolecular forms. As illustrated by the DOS diagrams, the models were in different conditions of electronic molecular orbitals levels not only for the exact HOMO and LUMO levels but for other levels before HOMO and after LUMO resulting in the possibility of detection of such complex formations. The results indicated variations of electronic molecular orbitals for all two models of bimolecular complexes compared to each other and the singular models. In this regard, the singular Frm had a long distance between HOMO and LUMO levels, as indicated by the energy gap values (EGap). Accordingly, the Fermi energy (EFermi) was placed in a different region compared to other models. After the formations of complexes, the models were found to be closer to the levels of the singular BN plate than the singular Frm model affirming the dominant role of BN plate in conducting the adsorption process. In this regard, the models were found to be in diagnostic levels compared to each other. The obtained features of chemical hardness and softness (CH and CS) also indicated different features for the models based on the obtained values of CH and CS among the investigating singular and bimolecular models. Consequently, the models were considered to cover the role of adsorption and provide a possibility of detecting the adsorbed substance. Indeed, the removal and diagnostic purposes could be proposed by employing a small BN plate towards the Frm substance.

4. Conclusions

A BN plate was investigated in this work for adsorbing the Frm substance by performing DFT calculations. To manage the adsorption process, one Fe atom was inserted in the center of the plate to make a Fe-doped BN plate for interacting with the Frm substance. Accordingly, two models of Frm@BN bimolecular complexes were found to be stable to

approach the goal of this work. The configurations of interactions of Frm substance towards the Fe-doped region were found to be through two orientations from O-leg and H-leg of Frm, resulting O…Fe and H…N interactions in F1 and H…Fe and H…N interactions in F2. Next, the obtained results of QTAIM analyses indicated the meaningful strengths of interactions for F1 and F2 models leading to higher stability for F1 in comparison with F2. The electronic molecular orbitals levels also affirmed the impacts of complex formations. The results were useful for approaching a diagnostic purpose of Frm substance with the assistance of a Fe-doped BN plate. Indeed, most of this work was to investigate a small-size model for adsorbing an environmental pollutant substance. The results indicated that the models were suitable for being achievable. The obtained interaction details and strengths also indicated the dominant role of BN in adsorbing the Frm substance regarding environmental issues.

Funding

This research received no external funding.

Acknowledgments

This research has no acknowledgment.

Conflicts of Interest

The authors declare no conflict of interest.

References

1. Ghanavati, B.; Bozorgian, A.; Kazemi Esfeh, H. Thermodynamic and kinetic study of adsorption of cobalt II using adsorbent of magnesium oxide nano-particles deposited on chitosan. *Progress in Chemical and Biochemical Research* **2022,** *5,* 165–181, https://doi.org/10.22034/pcbr.2022.335475.1219.
2. Ghanavati, B.; Bozorgian, A. Removal of copper II from industrial effluent with beta zeolite nanocrystals. *Progress in Chemical and Biochemical Research* **2022,** *5,* 53–67, https://doi.org/10.22034/pcbr.2022.328704.1213.
3. Al-Mutlaq, S.; Mahal, E. Synthesis of activated carbon from scrap tires with petroleum kerosene as a decomposition auxiliary agent. *Eurasian Chemical Communications* **2022,** *4,* 580–589, https://doi.org/10.22034/ecc.2022.316296.1268.
4. Al-Layla, A.; Fadhil, A. Removal of calcium over apricot shell derived activated carbon, kinetic and thermodynamic study. *Chemical Methodologies* **2022,** *6,* 10–23, https://doi.org/10.22034/CHEMM.2022.1.2.
5. Adole, V. Synthesis, antibacterial, antifungal and DFT studies on structural, electronic and chemical reactivity of (E)-7-((1H-Indol-3-yl)methylene)-1,2,6,7-tetrahydro-8H-indeno[5,4-b]furan-8-one. *Advanced Journal of Chemistry-Section A* **2021,** *4,* 175–187, https://doi.org/10.22034/ajca.2021.278047.1250.
6. Mortezagholi, B.; Movahed, E.; Fathi, A.; Soleimani, M.; Forutan Mirhosseini, A.; Zeini, N.; Khatami, M.; Naderifar, M.; Abedi Kiasari, B.; Zareanshahraki, M. Plantmediated synthesis of silver-doped zinc oxide nanoparticles and evaluation of their antimicrobial activity against bacteria cause tooth decay. *Microscopy Research and Technique* **2022,** *in press,* https://doi.org/10.1002/jemt.24207.
7. Wikantyasning, E.R.; Mutmainnah, M.; Cholisoh, Z.; Hairunisa, I.; Bakar, M.F.A.; Da'I, M. Preparation of hydrogel nanocomposite containing gold nanoparticles with unique swelling/deswelling properties. *Rasayan Journal of Chemistry* **2019,** *12,* 1857–1863, https://doi.org/10.31788/rjc.2019.1245209.
8. Wikantyasning, E.R.; Kalsum, U.; Nurfiani, S.; Da'i, M.; Cholisoh, Z. Allylamine-conjugated polyacrylic acid and gold nanoparticles for colorimetric detection of bacteria. *Materials Science Forum* **2021,** *1029,* 137–144, https://doi.org/10.4028/www.scientific.net/MSF.1029.137.
9. Alinezhad, H.; Hajiabbas Tabar Amiri, P.; Mohseni Tavakkoli, S.; Muhiebes, R.; Fakri Mustafa, Y. Progressive types of Fe3O4 nanoparticles and their hybrids as catalysts. *Journal of Chemical Reviews* **2022,** *4,* 288–312, https://doi.org/10.22034/jcr.2022.325255.1137.

10. Hasanpour, F.; Taei, M.; Fouladgar, M.; Salehi, M. Au nano dendrites/composition optimized Nd-dopped cobalt oxide as an efficient electrocatalyst for ethanol oxidation. *Journal of Applied Organometallic Chemistry* **2022,** *2*, 203–211, https://doi.org/10.22034/jaoc.2022.154984.
11. Khalili, A.; Dehno Khalaji, A.; Mokhtari, A.; Keyvanfard, M. Synthesis, characterization, and methyl green removal of epichlorohydrin crosslinked schiff base chitosan/Fe2O3 nanocomposite. *Progress in Chemical and Biochemical Research* **2021**, *4*, 392–402, https://doi.org/10.22034/pcbr.2021.290770.1192.
12. Abd Al-Zahra, A.; Al-Sammarraie, A. Synthesis and characterization of zinc Sulfide nanostructure by sol gel method. *Chemical Methodologies* **2022,** *6*, 67–73, https://doi.org/10.22034/chemm.2022.1.7.
13. Sanati, M.; Dehno Khalaji, A.; Mokhtari, A.; Keyvanfard, M. Fast removal of methyl green from aqueous solution by adsorption onto new modified chitosan schiff base. *Progress in Chemical and Biochemical Research* **2021,** *4*, 319–330, https://doi.org/10.22034/pcbr.2021.285530.1186.
14. Shahamatpour, M.; Tabatabaee Ghomsheh, S.; Maghsoudi, S.; Azizi, S. Fenton processes, adsorption and nano filtration in industrial wastewater treatment. *Progress in Chemical and Biochemical Research* **2021,** *4*, 32–43, https://doi.org/10.22034/pcbr.2021.118152.
15. Rida, Z.; Hassan, S.; Awad, S. Synthesis and characterization of new Inorganic complexes and evaluation their corrosion inhibiter. *Chemical Methodologies* **2022,** *6*, 347–356, https://doi.org/10.22034/chemm.2022.326331.1431.
16. Ahmed, M.; Dekhyl, A.; Alwan, L. Preparation and characterization of nano-carbon as an adsorbent for industrial water treatment. *Eurasian Chemical Communications* **2022,** *4*, 852–862, https://doi.org/10.22034/ecc.2022.332809.1356.
17. Abass, A.; Al-Sammarraie, A. Synthesis of new PbO-Fe2O3-polypyrrole hybrid nanocomposite to improve the structural, magnetic and electrical characteristics of lead oxide. *Chemical Methodologies* **2022,** *6*, 301–318, https://doi.org/10.22034/chemm.2022.328159.1433.
18. Janitabar Darzi, S.; Bastami, H. Au decorated mesoporous TiO2 as a high performance photocatalyst towards crystal violet dye. *Advanced Journal of Chemistry-Section A* **2022,** *5*, 22–30, https://doi.org/10.22034/ajca.2022.305643.1281.
19. Belhadri, M.; Mokhtar, A.; Bengueddach, A.; Sassi, M. Efficient adsorbent based on bentonite functionalized with 3-aminopropyltriethoxysilane for dyes removal from aqueous solutions. *Eurasian Chemical Communications* **2021,** *3*, 881–892, https://doi.org/10.22034/ecc.2021.305858.1240.
20. Mohammed, R.; Saleh, K. Conducting poly[N-(4-methoxy phenyl)maleamic acid]/metals oxides nanocomposites for corrosion protection and bioactivity applications. *Chemical Methodologies* **2022,** *6*, 74–82, https://doi.org/10.22034/chemm.2022.1.8.
21. Kim, J.H.; Pham, T.V.; Hwang, J.H.; Kim, C.S.; Kim, M.J. Boron nitride nanotubes, synthesis and applications. *Nano Convergence* **2018,** *5*, 17, https://doi.org/10.1186/s40580-018-0149-y.
22. Kilic, M.E.; Lee, K.R. Novel two-dimensional tetrahexagonal boron nitride with a sizable band gap and a sign-tunable Poisson's ratio. *Nanoscale* **2021,** *13*, 9303–9314, https://doi.org/10.1039/d1nr00734c.
23. Angizi, S.; Alem, S.A.; Azar, M.H.; Shayeganfar, F.; Manning, M.I.; Hatamie, A.; Pakdel, A.; Simchi, A. A comprehensive review on planar boron nitride nanomaterials, From 2D nanosheets towards 0D quantum dots. *Progress in Materials Science* **2022,** *124*, 100884, https://doi.org/10.1016/j.pmatsci.2021.100884.
24. Yadav, A.; Dindorkar, S.S.; Ramisetti, S.B. Adsorption behaviour of boron nitride nanosheets towards the positive, negative and the neutral antibiotics, insights from first principle studies. *Journal of Water Process Engineering* **2022,** *46*, 102555, https://doi.org/10.1016/j.jwpe.2021.102555.
25. Wan, L.; Liu, C.; Cao, D.; Sun, X.; Zhu, H. High phase change enthalpy enabled by nanocellulose enhanced shape stable boron nitride aerogel. *ACS Applied Polymer Materials* **2020,** *2*, 3001–3009, https://doi.org/10.1021/acsapm.0c00445.
26. Elias, C.; Fugallo, G.; Valvin, P.; L'Henoret, C.; Li, J.; Edgar, J.H.; Sottile, F.; Lazzeri, M.; Ouerghi, A.; Gil, B.; Cassabois, G. Flat bands and giant light-matter interaction in hexagonal boron nitride. *Physical Review Letters* **2021,** *127*, 137401, https://doi.org/10.1103/physrevlett.127.137401.
27. Hayat, A.; Sohail, M.; Hamdy, M.S.; Taha, T.A.; AlSalem, H.S.; Alenad, A.M.; Amin, M.A.; Shah, R.; Palamanit, A.; Khan, J.; Nawawi, W.I. Fabrication, characteristics, and applications of boron nitride and their composite nanomaterials. *Surfaces and Interfaces* **2022,** *29*, 101725, https://doi.org/10.1016/j.surfin.2022.101725.
28. Turiansky, M.E.; Wickramaratne, D.; Lyons, J.L.; Van de Walle, C.G. Prospects for n-type conductivity in cubic boron nitride. *Applied Physics Letters* **2021,** *119*, 162105, https://doi.org/10.1063/5.0069970.

29. Sharma, B.; Sharma, A.; Myung, J.H. Selective ppb-level NO2 gas sensor based on SnO2-boron nitride nanotubes. *Sensors and Actuators B: Chemical* **2021,** *331,* 129464, https://doi.org/10.1016/j.snb.2021.129464.
30. Mammadova, S.; Nasibova, A.; Khalilov, R.; Mehraliyeva, S.; Valiyeva, M.; Gojayev, A.; Zhdanov, R.; Eftekhari, A. Nanomaterials application in air pollution remediation. *Eurasian Chemical Communications* **2022,** *4*, 160–166, https://doi.org/10.22034/ecc.2022.315481.1265.
31. Oluwafemi, O.; Emeka, A.; Johnson, J.; Ilesanmi, O.; Oluwatosin, O. Adsorptive removal of doxycycline from aqueous solutions by unactivated carbon and acid activated carbon brewery waste grain. *Eurasian Chemical Communications* **2022,** *4*, 997–1011, https://doi.org/10.22034/ecc.2022.333291.1367.
32. Vardini, M.; Abbasi, N.; Kaviani, A.; Ahmadi, M.; Karimi, E. Graphite electrode potentiometric sensor modified by surface imprinted silica gel to measure valproic acid. *Chemical Methodologies* **2022,** *6,* 398–408, https://doi.org/10.22034/chemm.2022.328620.1437.
33. Hanafizadeh, P.; Karimi, A.; Taklifi, A.; Hojati, A. Experimental investigation of two-phase water–oil flow pressure drop in inclined pipes. Experimental Thermal and Fluid Science **2016,** *74,* 169–180, https://doi.org/10.1016/j.expthermflusci.2015.11.024.
34. Yaraghi, A.; Ozkendir, O.M.; Mirzaei, M. DFT studies of 5-fluorouracil tautomers on a silicon graphene nanosheet. *Superlattices and Microstructures* **2015,** *85,* 784–788, https://doi.org/10.1016/j.spmi.2015.05.053.
35. Ijuo, G.; Surma, N.; Igoli, J. Ag-nanoparticles mediated by lonchocarpus laxiflorus stem bark extract as anticorrosion additive for mild steel in 1.0 M HCl solution. *Progress in Chemical and Biochemical Research* **2022,** *5*, 133–146, https://doi.org/10.22034/pcbr.2022.324366.1208.
36. Muñoz, A.D.; Escobedo-Morales, A.; Skakerzadeh, E.; Anota, E.C. Effect of homonuclear boron bonds in the adsorption of DNA nucleobases on boron nitride nanosheets. *Journal of Molecular Liquids* **2021,** *322,* 114951, https://doi.org/10.1016/j.molliq.2020.114951.
37. Liu, X.; Ahmadi, Z. H2O and H2S adsorption by assistance of a heterogeneous carbon-boron-nitrogen nanocage: computational study. *Main Group Chemistry* **2022,** *21,* 185–193, https://doi.org/10.3233/mgc-210113.
38. Balali, E.; Davatgaran, S.; Sheikhi, M.; Shahab, S.; Kaviani, S. Adsorption of doxepin drug on the surface of B12N12 and Al12N12 nanoclusters: DFT and TD-DFT perspectives. *Main Group Chemistry* **2022,** *21,* 69–84, https://doi.org/10.3233/mgc-210083.
39. Chukwuanukwu, T.; Afiadigwe, E.; Apakama, A.; Chukwuanukwu, R.; Uchechukwu Nwankwo, E.; Ilokanuno, C. Epidemiology of cleft lip and palate in Nigeria: a data-based study. *International Journal of Scientific Research in Dental and Medical Sciences* **2021,** *3,* 73–77, https://doi.org/10.30485/ijsrdms.2021.278259.1137.
40. Ulasi, T.; Nri-Ezedi, C.; Ofiaeli, O.; Chijioke, E. Novel cases of diamond blackfan anaemia in two nigerian toddlers, roadmap for care in resource-limited nations. *International Journal of Scientific Research in Dental and Medical Sciences* **2021,** *3,* 101–104, https://doi.org/10.30485/ijsrdms.2021.282666.1148.
41. Cedeño, A.; Bustamante, G.; Castrillo, A.; Ramos, S. Mandibular plasmocytoma: a case report of a rare entity. *International Journal of Scientific Research in Dental and Medical Sciences* **2020,** *2,* 138–140, https://doi.org/10.30485/ijsrdms.2020.256693.1097.
42. Şahin, K.E.; Baglan Uzunget, S.; Keskinruzgar, A. Elastic properties of the aorta are affected in young patients with sleep bruxism. *International Journal of Scientific Research in Dental and Medical Sciences* **2021,** *3*, 171–178, https://doi.org/10.30485/ijsrdms.2021.315608.1216.
43. Nazneen, A. Scrotal defects reconstruction after fournier's gangrene. *International Journal of Scientific Research in Dental and Medical Sciences* **2021,** *3,* 184–187, https://doi.org/10.30485/ijsrdms.2021.315745.1217.
44. Salthammer, T. Formaldehyde sources, formaldehyde concentrations and air exchange rates in European housings. *Building and Environment* **2019,** *150,* 219–232, https://doi.org/10.1016/j.buildenv.2018.12.042.
45. Reingruber, H.; Pontel, L.B. Formaldehyde metabolism and its impact on human health. *Current Opinion in Toxicology* **2018,** *9,* 28-34, https://doi.org/10.1016/j.cotox.2018.07.001.
46. Kamps, J.J.; Hopkinson, R.J.; Schofield, C.J.; Claridge, T.D. How formaldehyde reacts with amino acids. *Communications Chemistry* **2019,** *2,* 126, https://doi.org/10.1038/s42004-019-0224-2.
47. Liu, C.; Huang, W.; Zhang, J.; Rao, Z.; Gu, Y.; Jérôme, F. Formaldehyde in multicomponent reactions. *Green Chemistry* **2021,** *23,* 1447–1465, https://doi.org/10.1039/d0gc04124f.

48. Brdarić, D.; Kovač-Andrić, E.; Šapina, M.; Kramarić, K.; Lutz, N.; Perković, T.; Egorov, A. Indoor air pollution with benzene, formaldehyde, and nitrogen dioxide in schools in Osijek, Croatia. *Air Quality, Atmosphere & Health* **2019,** *12*, 963–968, https://doi.org/10.1007/s11869-019-00715-7.
49. Yue, X.; Ma, N.L.; Sonne, C.; Guan, R.; Lam, S.S.; Van Le, Q.; Chen, X.; Yang, Y.; Gu, H.; Rinklebe, J.; Peng, W. Mitigation of indoor air pollution: a review of recent advances in adsorption materials and catalytic oxidation. *Journal of Hazardous Materials* **2021,** *405*, 124138, https://doi.org/10.1016/j.jhazmat.2020.124138.
50. Robert, B.; Nallathambi, G. Indoor formaldehyde removal by catalytic oxidation, adsorption and nanofibrous membranes, a review. *Environmental Chemistry Letters* **2021,** *19*, 2551–2579, https://doi.org/10.1007/s10311-020-01168-6.
51. Suresh, S.; Bandosz, T.J. Removal of formaldehyde on carbon-based materials: a review of the recent approaches and findings. *Carbon* **2018,** *137*, 207–221, https://doi.org/10.1016/j.carbon.2018.05.023.
52. Sahraian, M.A.; Shahmohammadi, A.; Shahmohammadi, S.; Doosti, R. Leukoencephalopathy with brain stem and spinal cord involvement and lactate elevation (LBSL) based on typical MRI and MRS findings: a case report. *International Journal of Scientific Research in Dental and Medical Sciences* **2022,** *4*, 38–41, https://doi.org/10.30485/ijsrdms.2022.325233.1241.
53. Soghli, N.; Panjnoush, M.; Johari, M. Incidental finding of a supernumerary tooth fused to a mandibular second molar using cone beam computed tomography (CBCT): a case report. *International Journal of Scientific Research in Dental and Medical Sciences* **2020,** *2*, 20–22, https://doi.org/10.30485/ijsrdms.2020.204662.1022.
54. Kaviani, M.; Kia, J. Determination of hepatitis B antibody titration and related factors in dental students in Guilan University of Medical Sciences. *International Journal of Scientific Research in Dental and Medical Sciences* **2019,** *1*, 40–47, https://doi.org/10.30485/ijsrdms.2019.195149.1011.
55. Zhang, W.; Chen, L.; Xu, L.; Dong, H.; Hu, H.; Xiao, Y.; Zheng, M.; Liu, Y.; Liang, Y. Advanced nanonetwork-structured carbon materials for high-performance formaldehyde capture. *Journal of Colloid and Interface Science* **2019,** *537*, 562–568, https://doi.org/10.1016/j.jcis.2018.11.047.
56. Oyeneyin, O.; Abayomi, T.; Ipinloju, N.; Agbaffa, E.; Akerele, D.; Arobadade, O. Investigation of amino chalcone derivatives as anti-proliferative agents against MCF-7 breast cancer cell lines - DFT, molecular docking and pharmacokinetics studies. *Advanced Journal of Chemistry-Section A* **2021,** *4*, 288–299, https://doi.org/10.22034/ajca.2021.285869.1261.
57. Farhami, N. A computational study of thiophene adsorption on boron nitride vanotube. *Journal of Applied Organometallic Chemistry* **2022,** *2*, 163–172, https://doi.org/10.22034/jaoc.2022.154821.
58. Anafcheh, M. A comparison between density functional theory calculations and the additive schemes of polarizabilities of the Li-F-decorated BN cages. *Journal of Applied Organometallic Chemistry* **2021,** *1*, 125–133, https://doi.org/10.22034/jaoc.2021.292384.1027.
59. Venkatesh, G.; Sheena Mary, Y.; Shymamary, Y.; Palanisamy, V.; Govindaraju, M. Quantum chemical and molecular docking studies of some phenothiazine derivatives. *Journal of Applied Organometallic Chemistry* **2021,** *1*, 148–158, https://doi.org/10.22034/jaoc.2021.303059.1033.
60. Ajala, A.; Uzairu, A.; Shallangwa, G.; Abechi, S. In-silico design, molecular docking and pharmacokinetics studies of some tacrine derivatives as anti-alzheimer agents, theoretical investigation. *Advanced Journal of Chemistry-Section A* **2022,** *5*, 59–69, https://doi.org/10.22034/ajca.2022.321171.1292.
61. Abdullahi, Y.Z. Antiferromagnetic semiconductor in porous boron nitride (B6N6) sheet, First-principles investigation. *Computational and Theoretical Chemistry* **2021,** *1197*, 113155, https://doi.org/10.1016/j.comptc.2021.113155.
62. Akinlosotu, O.; Ogunyemi, B.; Adeleke, B. Substituent effect on bithiophene-bipyridine organic conjugated systems, theoretical investigation. *Advanced Journal of Chemistry-Section A* **2022,** *5*, 70–80, https://doi.org/10.22034/ajca.2022.320173.1290.
63. Alwan, L.; Al Samarrai, E.; Mahmood, M.; Ali, Q.; Al Samarrai, O. Estimation and development of some biophysical characteristics of the drug favipiravir used in the treatment of corona-virus using green chemistry technology. *Eurasian Chemical Communications* **2022,** *4*, 835–851, https://doi.org/10.22034/ecc.2022.332743.1352.
64. Islam, J.; Kumer, A.; Chakma, U.; Alam, M.; Biswas, S.; Ahmad, Z.; Islam, M.; Jony, M.; Ahmed, M. Investigation of structural, electronic, and optical properties of SrTiO3 and SrTi0.94Ag0.06O3 quantum dots based semiconductor using first principle approach. *Advanced Journal of Chemistry-Section A* **2022,** *5*, 164–174, https://doi.org/10.22034/ajca.2022.325958.1300.

65. Ariaei, S.; Sakhaeinia, H.; Heydarinasab, A.; Shokouhi, M. CO and NO selective adsorption by a C16Mg8O8 nanocage: a DFT study. *Main Group Chemistry* **2021,** *20*, 489–499, https://doi.org/10.3233/mgc-210060.
66. Zarifi, K.; Rezaei, F.; Seyed Alizadeh, S.M. A model of FeN-decorated BeO layer particle for CO gas adsorption. *Main Group Chemistry* **2022,** *21*, 125–132, https://doi.org/10.3233/mgc-210100.
67. Frisch, M.J.; Trucks, G.W.; Schlegel, H.B.; Scuseria, G.E.; Robb, M.A.; Cheeseman, J.R. Gaussian 09 program. *Gaussian Inc. Wallingford*, CT, **2009**.
68. Parkan, A.; Mirzaei, M.; Tavakoli, N.; Homayouni, A. Molecular interactions of indomethacin and amino acids: computational approach. *Main Group Chemistry* **2022,** *21*, 611–621, https://doi.org/10.3233/mgc-210157.
69. Pour Karim, S.; Ahmadi, R.; Yousefi, M.; Kalateh, K.; Zarei, G. Interaction of graphene with amoxicillin antibiotic by in silico study. *Chemical Methodologies* **2022,** *6*, 861–871, https://doi.org/10.22034/chemm.2022.347571.1560.
70. Srivastava, A.K. Ionization of NO by superhalogens: DFT and QTAIM approaches. *Main Group Chemistry* **2021,** *20*, 33–40, https://doi.org/10.3233/mgc-210004.